High spatial resolution bidirectional reflectance retrieval using satellite data

Richard C. Olsen, Angela M. Kim, Cecelia McConnon

Naval Postgraduate School, Monterey, CA

ABSTRACT

Worldview-2 imagery acquired over Duck, NC and Camp Pendleton, CA were analyzed to extract Bidirectional Reflectance Distribution Functions (BRDF) for 8 visible/near-infrared spectral bands. Images were acquired at 15 azimuth/elevation positions at ten-second intervals during the Duck, NC orbit pass. Ten images were acquired over Camp Pendleton, CA. Orthoready images were coregistered using first-order polynomials for the two image sequences. BRDF profiles have been created for various scene elements. MODTRAN simulations are presented to illustrate atmospheric effects under varying collection geometries. Results from analysis of the Camp Pendleton, CA data are presented here.

Keywords: Bidirectional Reflectance Distribution Function, BRDF, WorldView-2

1. INTRODUCTION

The measured reflectance of a material varies depending upon the angle relative to the surface at which the measurement is taken, and the source of illumination. The Bidirectional Reflectance Distribution Function (BRDF) describes the scattering characteristics of a material or object by quantifying how light from a source is reflected in a given direction. An example of this effect is given in Figure 1. The data used in this graphic was collected by NASA's Multi-angle Imaging SpectroRadiometer (MISR). This sensor was launched in 1999, and has nine cameras that simultaneously image the Earth at nine discrete angles (reaching as far as 70 degrees off-nadir), in the blue, green, red and near-infrared spectral bands. Its spatial resolution ranges from 1 km to 275 m.

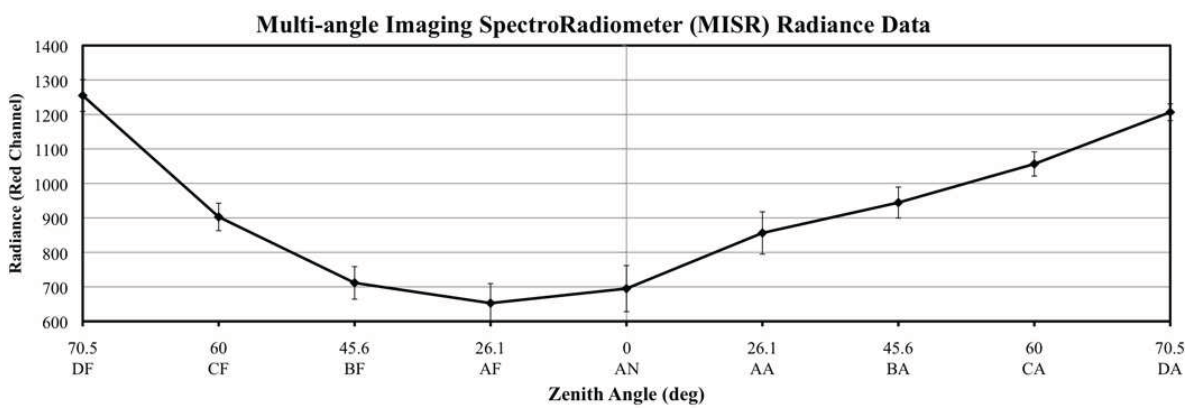

Figure 1. Radiance values for a region of interest (vegetated land cover) for multiple-angles as recorded by NASA's MISR sensor.

In addition to NASA's MISR instrument, multiple space-borne systems have demonstrated the existence of BRDF effects. Another set of NASA instruments, the Polarization and Directionality of the Earth's Reflectances

R.C.O.: E-mail: olsen@nps.edu, Telephone: 1 831 656 2019
A.M.K.: E-mail: amkim@nps.edu, Telephone: 1 831 656 3330

Algorithms and Technologies for Multispectral, Hyperspectral, and Ultraspectral Imagery XVII,
edited by Sylvia S. Shen, Paul E. Lewis, Proc. of SPIE Vol. 8048, 80480W · © 2011 SPIE
CCC code: 0277-786X/11/$18 · doi: 10.1117/12.883572

(POLDER) systems, were launched in 1996 and 2002. These systems used a wide FOV lens and a rotating filter and polarizing wheel to scan eight spectral bands in the visible and NIR range. BRDF was measured for viewing zenith angles up to 60 degrees for the full azimuth range, at a spatial resolution of approximately 6 km. A single pass of the satellite resulted in 14 successive images with various viewing angles. The European Space Agency launched the Compact High Resolution Imaging Spectrometer (CHRIS) system in 2001. This system acquires 13 spectral channels at 17 m resolution, or 62 spectral channels at 34 m resolution. The satellite has the ability to image a site five times during a single pass, and can view across-track, which reduces its revisit time to less than a week.

For the purposes of this study, data collected by the WorldView-2 (WV-2) satellite is used to investigate BRDF effects at finer spatial scales that was previously possible. The WV-2 satellite was launched in 2009, has a high spatial resolution ($\sim$ 0.5 m pan, <2 m multispectral), 8 spectral channels (see Table 1), and the capability to take rapid sequences of images ($\sim$ 10 s between images). Two multi-angular datasets were examined. The first dataset includes a sequence of 15 images collected over Duck, NC. The second dataset consists of 10 images acquired over Camp Pendleton, CA. This paper will focus on the results of the Camp Pendleton, CA study area. The varying azimuth/elevation angles for the Camp Pendleton collection are given in Table 2.

Table 1. WorldView-2 Spectral Channels[1]

Coastal	400 - 450 nm	Blue	450 - 510 nm
Green	510 - 580 nm	Yellow	585 - 625 nm
Red	630 - 690 nm	Red Edge	705 - 745 nm
Near-IR1	770 - 895 nm	Near-IR2	860 - 1040 nm

Table 2. Acquisition parameters - Pendleton, CA Dataset

Name	Acquisition Time (GMT)	Mean Sensor Azimuth (deg)	Mean Sensor Zenith (deg)	Solar Azimuth (deg)	Solar Elev. (deg)
1/P002	19:03:32	277.8	28.8	155.9	56.2
2/P007	19:03:42	267.1	29.9	156	56.2
3/P009	19:03:53	257.6	31.8	156.1	56.2
4/P006	19:04:04	249.5	34.2	156.2	56.3
5/P008	19:04:15	242.9	36.9	156.2	56.3
6/P004	19:04:26	237.3	39.9	156.3	56.3
7/P010	19:04:36	232.9	42.8	156.4	56.3
8/P005	19:04:47	229.2	45.6	156.5	56.3
9/P003	19:04:57	226.2	48.4	156.5	56.3
10/P001	19:05:08	223.6	50.9	156.6	56.3

2. METHODS

Limited pre-processing was applied to the imagery. The imagery was acquired from DigitalGlobe processed to Ortho-ready level 2A (OR2A). This processing includes radiometric and sensor correction to reduce the effects of noise in the imagery. The processing also provides a uniform GSD throughout the image and projects the image on a plane to a specified map projection and datum. The OR2A data is projected to an average elevation, but has no topographic relief applied, making it ready for custom ortho-rectification.[2] The ENVI software WorldView Radiance Calibration tool was used to convert the data from relative radiance into absolute radiance using the calibration factors in the WorldView-2 metadata files.[3]

2.1 Image Registration

The imagery was first coregistered using the image P008 as the base image. Image tie points were hand-selected, and first-order polynomials were used to warp the images to a common geographic reference system.

2.2 Image Ratios

Taking a ratio of images creates a product which only shows the relative difference between images. Figure 2 shows the ratio of the coastal band from P009 to P010. Bright areas are regions where P009 and P010 are very similar (ratio = 1.0). Dark areas represent areas of difference between the two images, and therefore a dependence on view angle. For comparison, the coastal band from P010 is shown in Figure 3.

As noted in Table 2, P010 was acquired approximately one minute after P009 during the same satellite overpass. The location of the sun relative to the sensor and scene changed very little in this time, so the differences between P009 and P010 represented by the darker regions in the ratio image are therefore due to the change view angle of the sensor (sensor zenith changes from 31.8 to 42.8 degrees, and azimuth changes from 257.6 to 232.9 degrees).

2.3 Regions of Interest

Regions of interest (ROIs) were selected representing the major ground-cover classes to include a selection of natural and man-made materials. Three of these regions (field, soil (wet) and soil (dry) are contained in the image chip shown in Figure 3.

- Ocean
- Harbor
- Marsh (Veg)
- Field (Veg)
- Soil (Wet and Dry)
- Sand (Three Types)
- Tarmac

The n-D visualizer tool in the ENVI software, which creates a multidimensional scatterplot in spectral space, was used to remove the outlying pixels from the ROIs to ensure the selected regions represented "pure" materials.[3]

Figure 2. Ratio of subset of Coastal bands (400-450 nm) from P009 and P010, Camp Pendleton, CA.

Figure 3. Subset of Coastal band (400-450 nm) from P010, Camp Pendleton, CA, with Regions of Interest outlined in white.

3. OBSERVATIONS AND ANALYSIS

3.1 Regions of Interest

The ratio of P009 to P010 as illustrated for a single band in Figure 2, shows that different material classes are affected differently by changing collection geometry. By looking at the mean value of each ROI for all bands in the ratio images, it can be seen that this dependence upon collection geometry is also wavelength dependent. Figure 4 shows the mean value of each of the ROIs for the ratio of image P009 to P010.

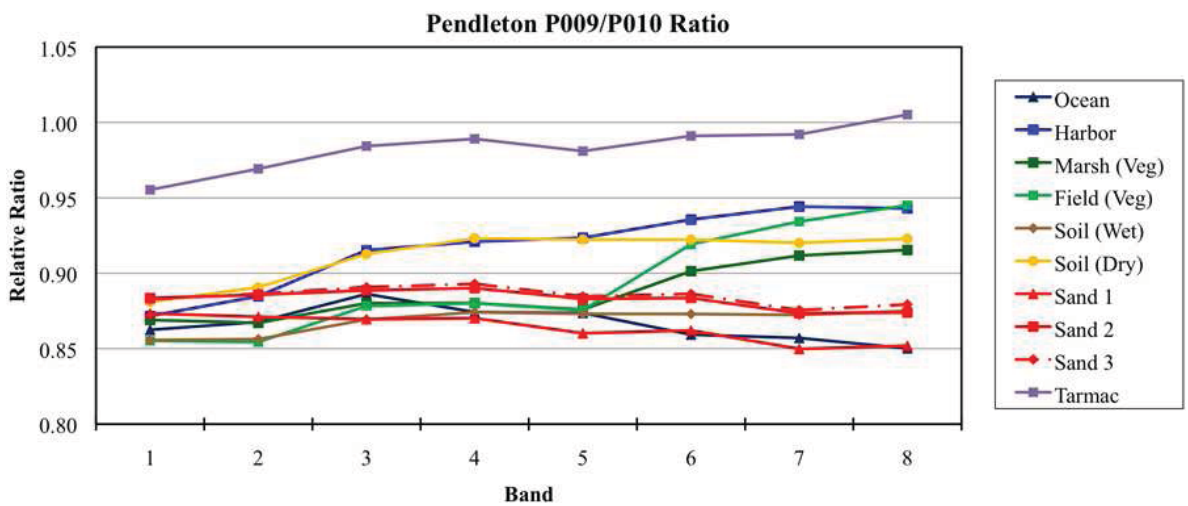

Figure 4. Mean ROI values for regions of the ratio images.

For each of the ROIs, the mean value of the region for each image was calculated, and normalized versus the mean ROI value for P002. These values are plotted versus sensor zenith angle in Figure 5.

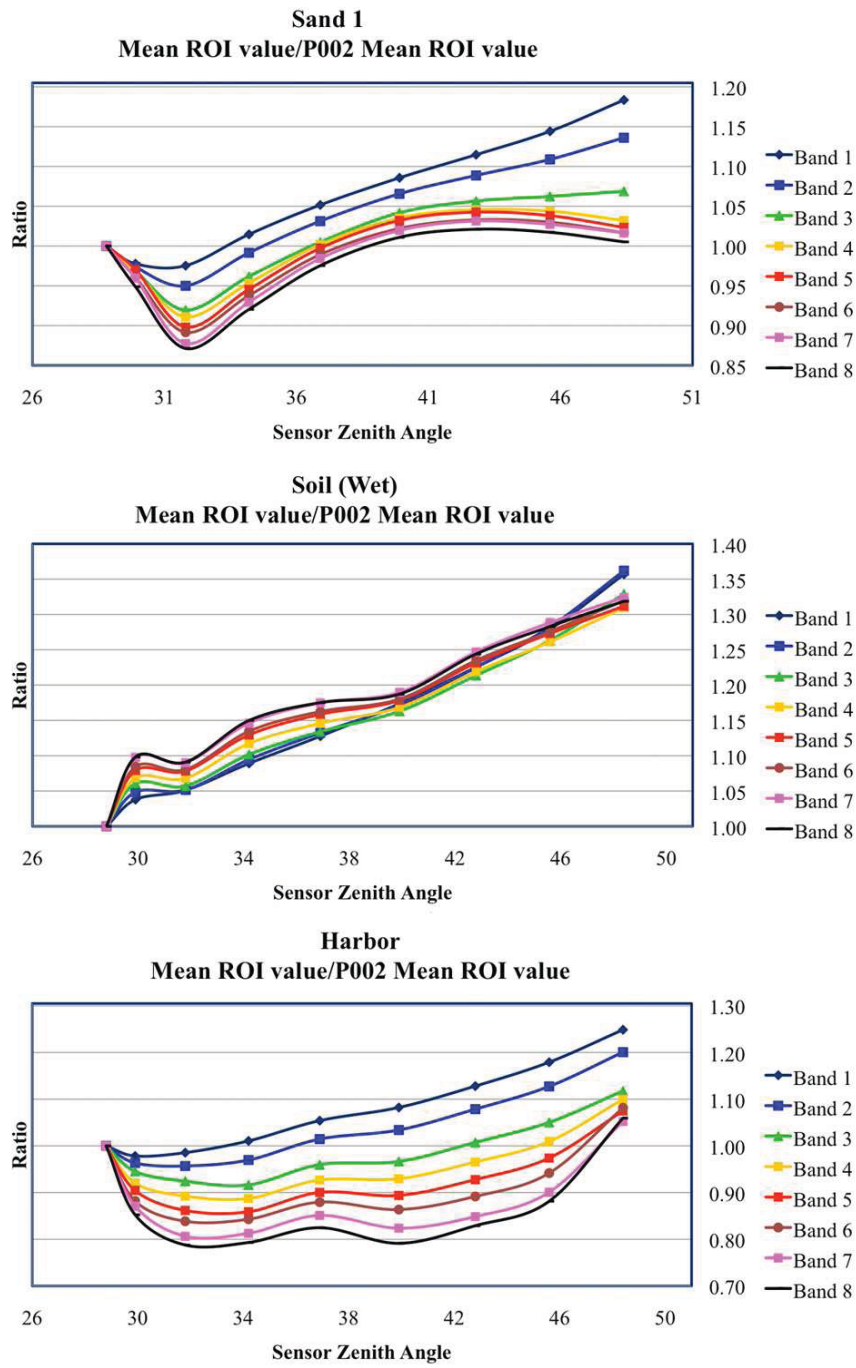

Figure 5. Mean Region of Interest values, normalized by dividing by the mean P002 ROI value, plotted versus sensor zenith angle.

3.2 Histograms

Histograms were created showing the distribution of brightness values within each spectral channel. Figures 6, 7, and 8 are plots of the histograms of the Pendleton, CA time-series images for three spectral channels. These figures illustrate how the distribution of brightness values shifts as the viewing geometry changes, and demonstrate that there is a variation in dynamic range with viewing geometry which is wavelength dependent. Some

of the variation present in 400-450nm band (Figure 6) could depend on aerosols, whereas in the 630-690nm and 770-895nm channels, the atmosphere has less of an effect.

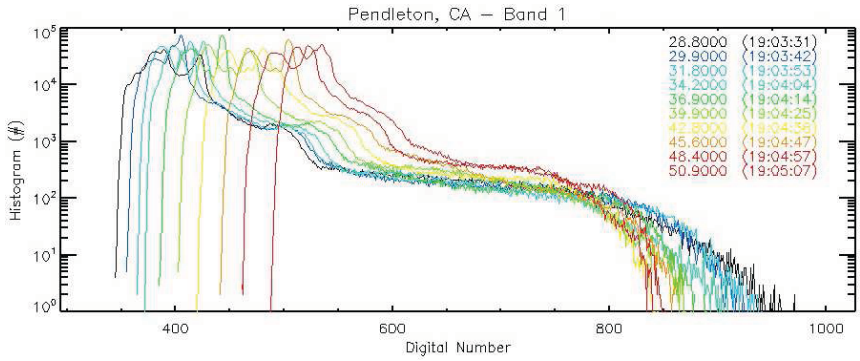

Figure 6. Histograms of brightness values for spectral channel 1 (400-450 nm) for time-series images. Images ordered by sensor zenith angle, with the image acquisition time given in parentheses.

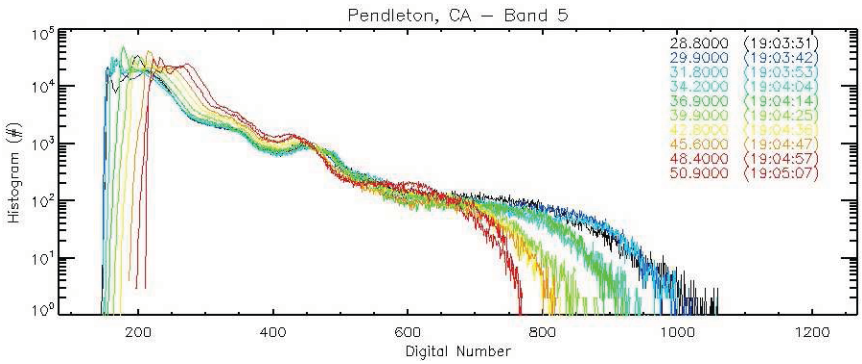

Figure 7. Histograms of brightness values for spectral channel 5 (630-690 nm) for time-series images. Images ordered by sensor zenith angle, with the image acquisition time given in parentheses.

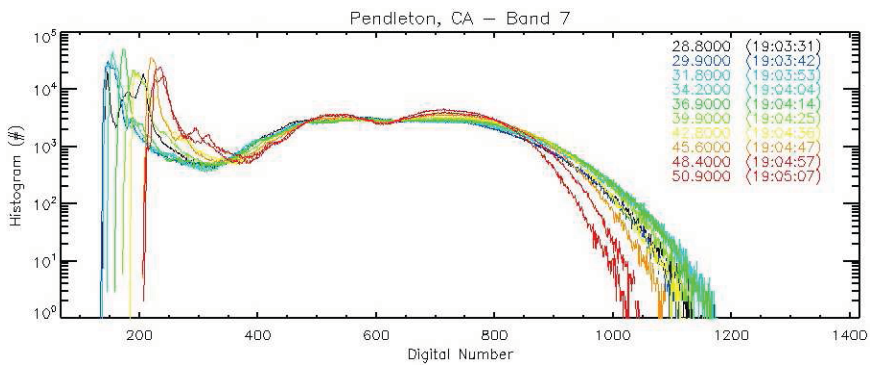

Figure 8. Histograms of brightness values for spectral channel 7 (770-895 nm) for time-series images. Images ordered by separation angle, with the image acquisition time given in parentheses.

4. MODTRAN SIMULATIONS

The MODTRAN radiative transfer code was used to simulate radiance data under conditions similar to those of the Camp Pendleton collect.[4] These simulations allow deductions to be made about the influences of the atmosphere on the recorded data, and therefore allow the separation of atmospheric effects from BRDF effects. A version of the U.S. Standard atmosphere, modified to incorporate increased atmospheric loading, was used in these simulations. The location of the sun and the satellite azimuth angle were held constant across all of the simulations; the only variation is the satellite zenith angle.

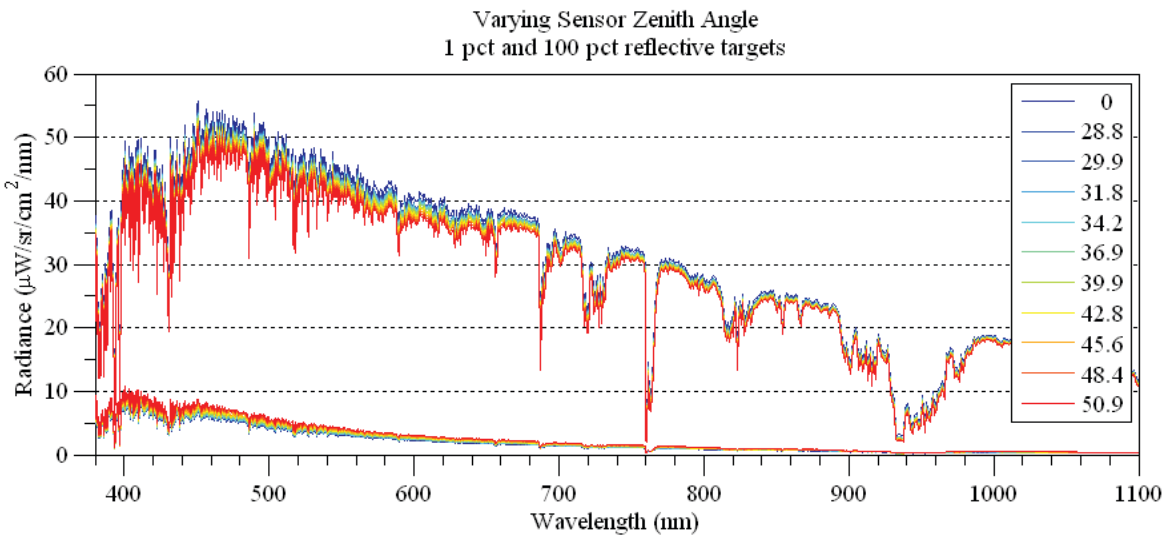

Figure 9. MODTRAN simulated radiance values of a dark (1% reflective) and a bright (100% reflective) target.

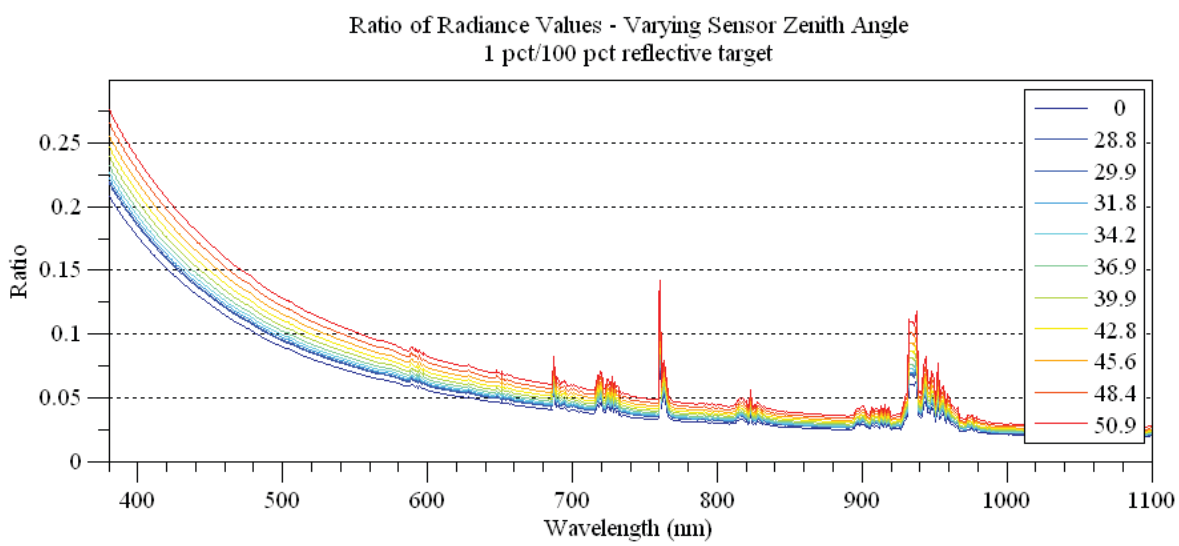

Figure 10. Ratio of MODTRAN simulated radiance values of a dark (1% reflective) to a bright (100% reflective) target.

5. CONCLUSIONS

The ability to collect multiple images in a very short time sequence during a single satellite overpass offers promise. BRDF effects are apparent in the datasets analyzed, but these effects are difficult to separate from the atmospheric effects.

REFERENCES

1. DigitalGlobe, Inc., "Worldview-2 Spacecraft Data Sheet." Downloaded from http://www.digitalglobe.com, January 2011.
2. DigitalGlobe, Inc., "DigitalGlobe Core Imagery Product Guide." Downloaded from http://www.digitalglobe.com, January 2010.
3. ITT Visual Information Solutions, "ENVI Help System." Distributed with ENVI software, 2011.
4. A. Berk, G. Anderson, P. Acharya, and E. Shettle, "MODTRAN 5.2.0.0 users's manual," tech. rep., Spectral Sciences, Inc, Air Force Research Laboratory, and Naval Research Laboratory, July 2008.